Polymer Degradation and Stability 99 (2014) 127–135

Contents lists available at ScienceDirect

Polymer Degradation and Stability

journal homepage: www.elsevier.com/locate/polydegstab

Influence of organically modified clays on the properties and disintegrability in compost of solution cast poly(3-hydroxybutyrate) films

D. Puglia [a,*], E. Fortunati [a], D.A. D'Amico [b], L.B. Manfredi [b], V.P. Cyras [b], J.M. Kenny [a,c]

[a] University of Perugia, Civil and Environmental Engineering Department, UdR INSTM, Strada di Pentima 4, 05100 Terni, Italy
[b] INTEMA – Instituto de Investigaciones en Ciencia y Tecnología de Materiales, Facultad de Ingeniería, Universidad Nacional de Mar del Plata, J. B. Justo 4302, Mar del Plata, Argentina
[c] Instituto de Ciencia y Tecnología de Polímeros, ICTP-CSIC, Juan de la Cierva 3, 28006 Madrid, Spain

ARTICLE INFO

Article history:
Received 12 June 2013
Received in revised form
21 October 2013
Accepted 24 November 2013
Available online 4 December 2013

Keywords:
Poly(hydroxybutyrate)
Nanoclay
Organic modification
Nanocomposites
Disintegrability
Compost

ABSTRACT

Polymer nanocomposites, based on a bacterial biodegradable thermoplastic polyester, poly(hydroxybutyrate) (PHB), and unmodified montmorillonite Cloisite Na^+ (CNa) and chemically modified Cloisite 15A and 93A (C15A and C93A), were prepared through a solution route. The nanostructure has been established through X-ray diffraction (XRD), while the nanocomposites were characterized by differential scanning calorimetry (DSC), contact angle measurements, and thermogravimetric (TGA) analysis. Disintegrability in composting conditions has been tested at certain times (0, 7, 14, 21, 28 and 35 days at 58 °C) and the effect of different nanoclays on the properties of biodegraded films was deeply investigated. XRD results suggest a better dispersion for C15A and C93A based nanocomposites that present also a more surface hydrophobic nature respect to PHB matrix and PHB nanocomposite loaded with unmodified Cloisite. This result is in accord with disintegrability behavior of PHB nanocomposites. Visual observation, chemical, thermal and morphological investigations proved that the disintegration in composting conditions was faster for PHB_4CNa respect to the systems loaded with modified clays suggesting the possibility to modulate the disintegrability capacity of PHB selecting a specific filler.

1. Introduction

The quantity of plastic waste is increasing every year and the precise time needed for biodegradation is unknown. Environmental awareness has driven the development of new biodegradable materials, especially for single use plastic items. Polyhydroxybutyrate (PHB) is a biodegradable thermoplastic polyester accumulated as an energy/carbon storage or reducing power material by numerous micro-organisms under unfavorable growth conditions in the presence of excess carbon source [1]. PHB is a partially crystalline polymer with a high melting temperature and a high degree of crystallinity, then it is brittle and has limited applications [2]; moreover, it is still much more expensive and lacks mechanical strength compared with conventional plastics. If the properties of the PHB can be further improved by the addition of a small quantity of an environmentally benign material, this polymer will find applications in more special or severe circumstances; in this case, it will be also necessary to know its behavior to degrade in similar to the real disposal waste. Preparation of nanocomposites represent a good alternative for reducing the final cost and an effective alternative way to acquire a new material with desired and improved properties of native biodegradable polymers such as thermal, mechanical and oxidative barrier. Montmorillonite is among the most commonly used clay because it is environmentally friendly and readily available in large quantities with relatively low cost [3,4]. Addition of nanoparticles such as nanoclays to form nanocomposites [5,6] has provided the means to improve materials performance including biodegradation. One advantage of clay nanocomposites is their capacity to improve polymer barrier properties retaining the flexibility and optical clarity of the pure matrix [7,8]. Incorporation of an organic modifier onto the clay surface, to mediate between the polarity of the hydrophilic clay surface and that of the more hydrophobic polymer, has been widely adopted for compatibilization and for easy exfoliation of the clay platelets into the polymer matrix during processing. Thus, as expected, the organoclay dispersibility within a polymer matrix has been found to depend on factors such as type and quantity of surfactant, type of clay, as well as on the processing conditions. It is reported that with only a few percent of clay,

* Corresponding author. Tel.: +39 (0) 744492916.
E-mail addresses: debora.puglia@gmail.com, debora.puglia@unipg.it (D. Puglia).

0141-3910/$ – see front matter © 2013 Elsevier Ltd. All rights reserved.
http://dx.doi.org/10.1016/j.polymdegradstab.2013.11.013

PHB exhibits greatly improved mechanical, thermal and barrier properties compared with the pristine polymers [9]. Recently, biodegradable aliphatic polyester nanocomposites obtained by using melt processing have been reported in the literature [10–12], while few example of solvent cast nanocomposites of PHB with organically modified montmorillonite having as surfactant organic quaternary ammonium salts have been previously reported [13]. These solution cast composites displayed intercalated morphologies and exhibited improved thermal stability, except for contents of clay in excess of 6 wt%. Since a notable characteristic of PHB is its biodegradability in the environment, many papers deal with the degradation in compost of PHAs [14–16]. Specifically, biodegradation of polyhydroxyalkanoate nanocomposites was first reported by Maiti and his colleagues in 2003 [17], in which melt extruded nanocomposites based on organically modified showed a well-ordered intercalated structure and severe degradation tendency, with increase in biodegradation rate due to the presence of acid sites which catalyze the hydrolysis of the ester linkages. The biodegradation of PHB and its nanocomposites with montmorillonite clay was also studied by Maiti et al. [18]. In this case the biodegradation rate in presence of montmorillonite was studied at room temperature and at 60 °C (under and above the glass transition of the matrix) and the results confirmed that, at the two different temperatures, silicate reinforced PHB nanocomposites showed higher degradation rate with respect of neat PHB. Nevertheless, reduced biodegradability of polymer in presence of specific nanoparticle was also reported in the literature [19]. However, few reports exist on the influence of different nanoparticles (carbon nanotubes [20], carbon nanofiber [21] and graphene [22,23]) on the degradation behavior of PHB (and copolymers) nanocomposites obtained by solvent assisted processing and also in the case of solvent cast PHB/montmorillonite nanocomposites, few papers analyzed the behavior in compost of such materials [10,24–26].

In this research, we report the preparation of polymer nanocomposites based on a bacterial biodegradable thermoplastic polyester, poly(hydroxybutyrate) (PHB) loaded with 4 wt% of unmodified montmorillonite Cloisite Na^+ (CNa) and chemically modified Cloisite 15A and 93A (C15A and C93A), prepared by a solution process. The nanostructure and the dispersion of the clay in polymer matrix has been established through X-ray diffraction, while the nanocomposites were characterized by differential scanning calorimetry (DSC), contact angle measurements, and thermogravimetric (TGA) analysis. Disintegrability in composting conditions of the materials has been tested at different times (0, 7, 14, 21, 28 and 35 days at 58 °C) and the effect of different nanoclays and mainly the influence of their modification on the properties of biodegraded films were analyzed by morphological, thermal and chemical investigations.

2. Experimental part

2.1. Materials

Polyhydroxybutyrate (PHB), with M_n = 250,000g/mol, was kindly supplied in pellets form by PHB Industrial S. A., Brazil. Unmodified montmorillonite (MMT) Cloisite Na^+, and two organically modified (OMMT) ones, Cloisite C15A and Cloisite C93A, were supplied by Southern Clay Products (Texas, USA). The characteristics of the clays are shown in Table 1. PHB films were obtained by casting process in chloroform and stirred at 450 rpm (15 min) at 60 °C. The obtained solution was placed on glass Petri dishes and it was allowed to evaporate at room temperature. Nanocomposites were prepared following the same procedure, but a chloroform clay solution, previously sonicated, was added to the PHB solution. All nanocomposite films, containing 4 wt% of each type of montmorillonite (named PHB_4CNa, PHB_4C15A and PHB_4C93A), were stored in a desiccator at room temperature for 30 days to allow complete crystallization of PHB [27]. The film thickness was 0.05 mm.

Table 1
Organic modifier and the interlayer distance of the clays.

	Cloisite® Na+ (CNa^+)	Cloisite® 93A (C93A)	Cloisite®15A (C15A)
Organic modifier	–	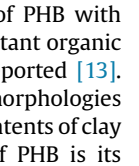	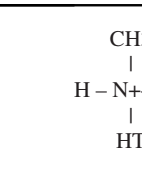
d(001)	11.7 Å	23.6 Å	31.5 Å

2.2. Methods

2.2.1. X-ray diffraction analysis (XRD)

A Philips PW 1710 X-ray diffractometer system with KCuα (λ = 1.54 Å) radiation was used to perform XRD analyses. Scans were recorded in the range of $2\theta = 2–36°$ at 2°/min with an X-ray tube operated at 45 kV and 30 mA.

2.2.2. Contact angle

The sessile drop method was used to determine the static contact angle of the films. Drops of 5 μl of doubly distilled water were placed on the material surfaces. Measures were done over six drops for each sample with a Ramé Hart model 500 Advanced Contact Angle Goniometer/Tensiometer equipped with the DROP image Advanced Software.

2.2.3. Differential scanning calorimetry (DSC)

Differential scanning calorimetric (DSC) experiments were performed on a Mettler Toledo 822e, in the temperature range from −25–200 °C, at a rate of 10 °C/min and under inert nitrogen atmosphere. Melting temperature (T_m) was determined as the maximum of the endothermic signal from the heating scan.

The overall crystallinity was calculated according to the equation (1):

$$Xc(\%) = \frac{\Delta H_m \cdot (m_C/m_P)}{\Delta H_0} \cdot 100 \quad (1)$$

where ΔH_m is the melting enthalpy measured from heating experiments, ΔH_0 is the theoretical enthalpy of 100% crystalline PHB (ΔH_0 = 146 J/g) [28], m_c is the nanocomposite weight and m_p is the weight of PHB in the nanocomposite.

2.2.4. Thermogravimetric analysis (TGA)

Thermal degradation measurements were carried out using a Seiko Exstar 6300 TGA/DTA system under nitrogen atmosphere (flow rate 250 ml/min). Temperature programs were run from 20 to 600 °C at 10 °C/min heating rate. The sample weight in each run was approximately 10 mg.

2.2.5. Disintegrability in composting conditions

Disintegrability of neat PHB and PHB composite films was observed by means of a disintegration test in composting conditions according to the ISO 20200 standard. A specific quantity of compost, inoculum supplied by Gesenu S.p.a., was mixed with the synthetic biowaste, and certain amount of sawdust, rabbit food,

starch, sugar, oil, and urea. The water content of the substrate was around 50 wt% and the aerobic conditions were guaranteed by mixing it softly. The samples cut to have approximately 15 × 15 × 0.05 mm^3 specimens were then buried in perforated boxes, containing the prepared mix, and incubated at 58 °C. The samples were recovered at different disintegration steps, washed with distilled water, dried in oven at 37 °C for 24 h, and weighed. The disintegrability value was obtained normalizing the sample weight, at different stages of incubation, to the initial one. Surface microstructure of PHB and PHB composites before the composting and at 7, 14, 21, 28 and 35 days of incubation was investigated by field emission scanning electron microscopy (FESEM, Supra 25-Zeiss) while sample photographs were taken for visual comparison. The samples at the different times of incubation were characterized by DSC, TGA using the test conditions described previously. Spectra were recorded with a Jasco FT-IR 615 spectrometer, in attenuated total reflection (ATR) mode. Spectra were collected at wavenumber values between 4000 and 400 cm^{-1} with spectral resolution of 4 $cm^{-}1$ while an average of 150 scans was considered.

3. Results and discussion

3.1. Characterization of PHB nanocomposite films

X-ray diffraction analyses were performed on the neat PHB and PHB nanocomposite films in order to investigate the dispersion of the montmorillonite layers in the polymer as well as to compare the PHB crystallinity in the materials. The spectra of the nanocomposites (Fig. 1) showed the same well-defined characteristics peaks of PHB [28,29], that remain practically unchanged. This fact suggests that the PHB crystalline lattice does not change appreciably in the presence of the different montmorillonites. The (001) diffraction peak of the clays, indicative of the interlayers distance, was observed in the low angles region of the nanocomposites spectra. It was observed a displacement of these characteristic peaks to lower angles when they were added to the PHB, taking as a reference the intergallery distance of the each pristine clay. An increase in the spacing between the layers, namely a peak shift to lower angles, is termed as an increase in degree of exfoliation [10,30,31]. The composites with C15A and C93A seemed to have structures that were better dispersed than the composite with CNa. The high hydrophilic character of CNa could be the reason of its poor dispersion in the polymer. A similar observation was reported by Pluta et al. [32] on PLA/CNa microcomposites. The composite containing the clay C93A showed a higher peak in the spectra region between 2° and 5°, than the one with C15A. It could suggest that most of the C15A clay has an interlayer distance higher than 44.12 Å ($2\theta = 2°$), which cannot be observed in the spectra.

The surface polarity of the different nanocomposites was also investigated measuring the contact angle of a drop of water on the films, with the aim of critically discussing the behavior of PHB nanocomposites during the degradation test in composting conditions. A plot of the measured water contact angle for the PHB neat films and for PHB based nanocomposite films was given in Fig. 2 (with enclosed images of the obtained experimental angles). As expected, PHB showed a hydrophobic character due to the poor affinity of the water to the non-polar polymer surface, giving a high contact angle (Fig. 2). A lower angle was observed in the drop when it was placed on the nanocomposite films containing CNa, due to the hydrophilic character of the unmodified MMT. On the other hand, the composites containing the organically modified MMT (OMMT) showed a higher hydrophobic nature than the PHB, because of the non-polar modifiers added to C15A and C93A clays [33]. Therefore, as shown in the following sections, this variation in the surface polarity of the films will influence the degradation behavior of the different materials in composting conditions.

Thermal behavior of PHB films and its nanocomposites was studied from the dynamic DSC thermograms. The crystallization temperature (T_c), the melting temperature (T_{m1}, T_{m2}), the cold crystallization temperature (T_{cc}) and related enthalpies (ΔH_{cc} and ΔH_m), such as the percentage of crystallinity (X_c), of the different materials were calculated and reported in Table 2, while in Fig. 3 the heat flow curves of cooling (Fig. 3a) and second heating scans (Fig. 3b) are reported for all the investigated systems. As observed in Fig. 3a, the addition and dispersion of clay into the matrix makes the crystallization occuring faster, and the result is consistent with previous reported studies on the addition of nucleating agents on PHB matrix [5]. Another phenomenon that has been observed is the appearance of double melting endotherms during melting. This behavior can be attributed to the well-known recrystallization phenomenon [34]. The lower temperature peak (T_{m1}) at about (169.9 ± 1.4) °C for PHB neat film corresponds to the melting of the

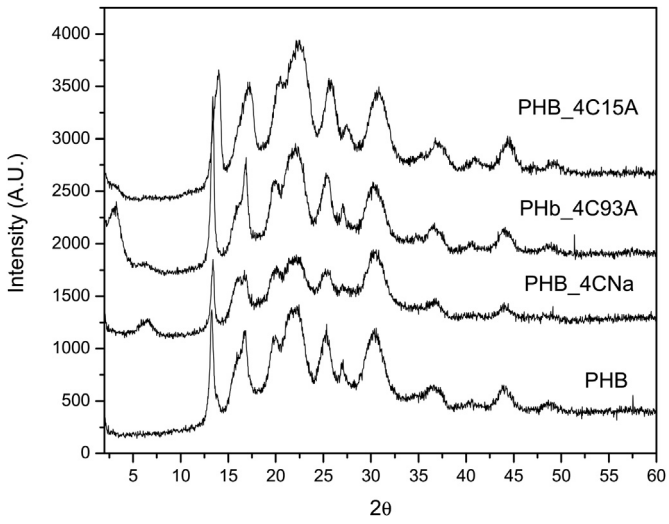

Fig. 1. X-ray diffraction spectra of neat PHB and PHB nanocomposite films.

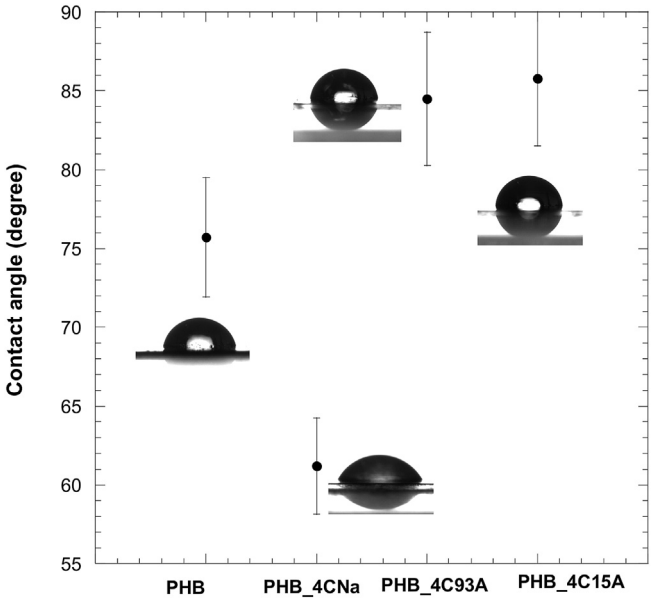

Fig. 2. Water contact angle values of PHB and PHB nanocomposite films.

Table 2
Thermal characteristics calculated for the PHB and its nanocomposites from DSC thermograms (cooling and 2nd heating scan).

	Cooling scan		2nd heating scan						TGA	
	ΔH_c (J/g)	T_c (°C)	T_{cc} (°C)	ΔH_{cc} (J/g)	ΔH_m (J/g)	T_{m1} (°C)	T_{m2} (°C)	X_m (%)	T_{peak} (°C)	Residual mass (%) @ 600 °C
PHB	68.9 ± 2.7	72.0 ± 0.9	90.3 ± 0.5	14.2 ± 1.8	93.5±1.4	169.9 ± 1.4	173.8 ± 0.2	54.3 ± 2.2	266.9 ± 2.0	0.58
PHB_4CNa	60.9 ± 5.2	74.0 ± 1.2	88.1 ± 0.1	8.1 ± 0.4	77.0 ± 7.6	157.5 ± 1.9	167.7 ± 0.8	45.3 ± 5.2	262.5 ± 1.0	6.08
PHB_4C15A	71.3 ± 6.2	71.7 ± 1.1	88.4 ± 1.5	13.1 ± 2.2	87.6 ± 6.4	155.7 ± 0.2	166.8 ± 1.0	49.0 ± 5.7	271.4 ± 1.5	3.67
PHB_4C93A	67.5 ± 3.7	80.9 ± 0.6	85.9 ± 6.4	10.4 ± 4.9	85.4 ± 2.6	169.0 ± 0.7	171.8 ± 2.2	49.3 ± 1.5	275.8 ± 2.0	2.08

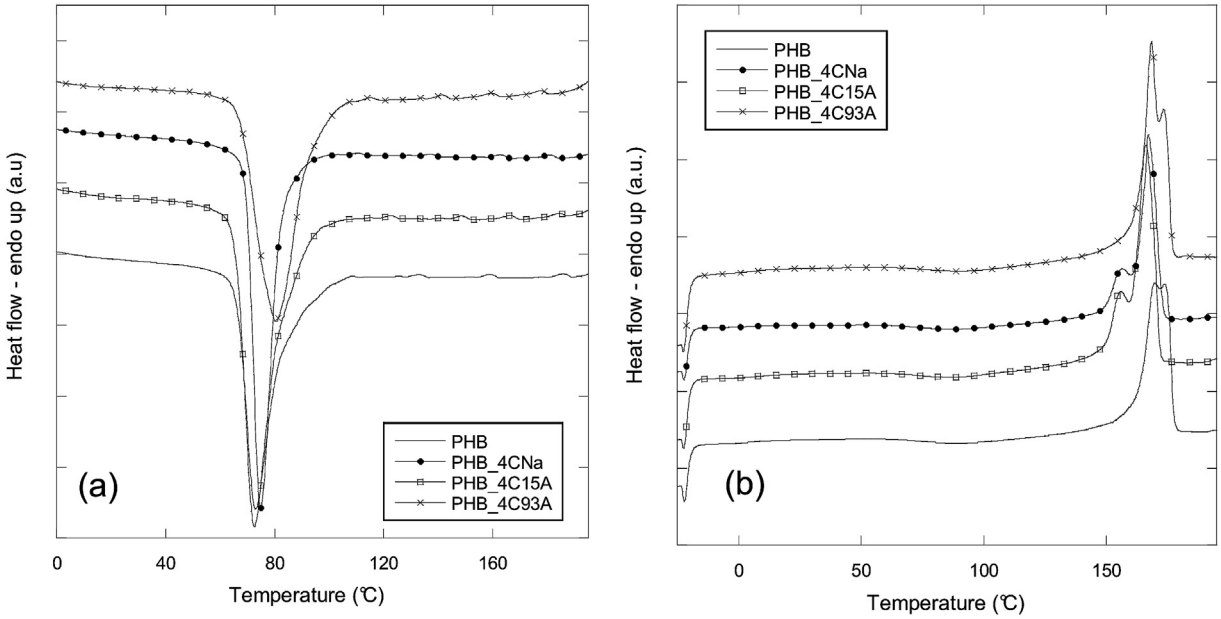

Fig. 3. DSC thermograms of PHB and PHB nanocomposites during the cooling (a) and the second heating (b) scan.

"as-formed" polymer crystals, while the higher temperature, T_{m2} = (173.8 ± 0.2) °C, corresponds to the melting of the PHB crystals formed from the recrystallization during the heating process. PHB_4C93A shows a similar behavior respect to the PHB neat film (Fig. 3b and Table 2) with no significant effect on the melting temperatures induced by the Cloisite 93A, while a shift to lower T_{m1} and T_{m2} was detected for both PHB_4CNa and PHB_4C15A nanocomposites probably due to a reduced crystallite size [35,36]. This behavior underlined an hindering effect of clay sheets on the recrystallization phenomenon for PHB_4CNa and PHB_4C15A systems, while PHB_4C93A showed improved recrystallization phenomena during melting confirmed by the increased mean value of crystallinity degree of C93A containing system with respect to the C15A and CNa^+, in which a reduction of the final X_m value was observed. Such phenomenon of clay platelets hindering crystal growth while enhancing nucleation step has already been observed in other nano-biocomposite systems [37,38].

Thermal degradation analysis was also performed in order to determine the influence of the clay addition on the thermal behavior of PHB. The residual mass vs temperature curves of PHB and PHB nanocomposite films are shown in Fig. 4a, while the derivative curves are reported in Fig. 4b. It was observed that the nanocomposites showed higher residual mass than the PHB, due to the presence of inorganic compounds (Fig. 4a and Table 2): specifically, the nanocomposites with CNa showed higher amount of residual mass than the other nanocomposites (Table 2). The DTG curve of PHB showed a peak at about 260 °C due to the polymer decomposition. This peak shifted to higher temperatures for the nanocomposites with OMMT, indicating that the introduction of this type of fillers slightly improve the thermal stability of PHB, acting as thermal barriers. On the contrary, in the case of CNa, the thermal resistance of PHB slightly decreased, due to the catalytic activity of the Al Lewis acid sites of MMT [36].

3.2. Disintegrability in composting of PHB nanocomposite films

Disintegrability in composting conditions was first evaluated by visual observation of the PHB and PHB nanocomposites at different times of incubation. Fig. 5 shows that all samples changed their color (in the web version) and became opaque after 7 days of incubation, while they exhibited a considerable surface deformation and fractures starting from 14 days in composting. This effect was more evident in the case of neat PHB after 14 days of incubation. The changes in sample color is a consequence of water absorption and/or presence of products formed by the hydrolytic process that induced a change in the refraction index of the specimens [39]. The visual observation highlighted that all the materials were visibly disintegrated after 28 days, while only PHB_4C15A and PHB_4C93A formulations were still present at 35 days in composting. This result is confirmed by disintegrability values (Fig. 6) that remain constant for all systems until 14 days of incubation, while a 25% at 21 days and a 95% at 28 days of disintegrability was detected for neat PHB film. A different behavior is detected for PHB nanocomposites, for which a visible mass loss is detected only after 28 days. During the initial phases of the disintegration, the high-molecular weight PHB chains are hydrolyzed to form lower molecular weight chains and this reaction can be delayed by the presence of organo-modified clays. They hinder the segmental motion of the PHB chains and

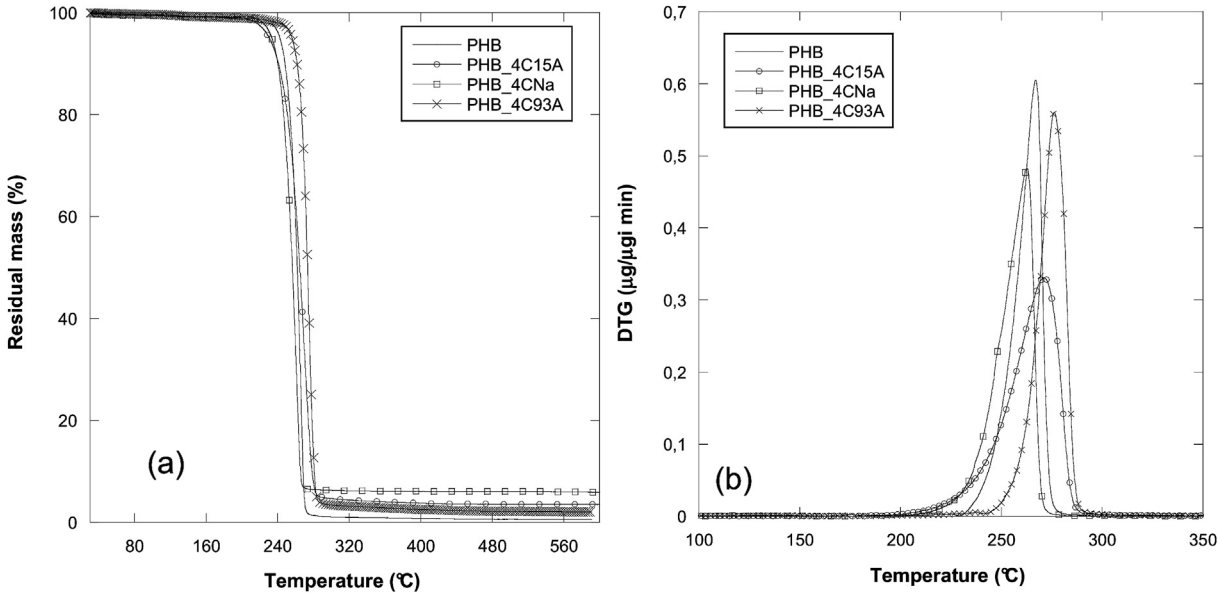

Fig. 4. Residual mass (a) and derivative curves (b) of PHB and PHB nanocomposites.

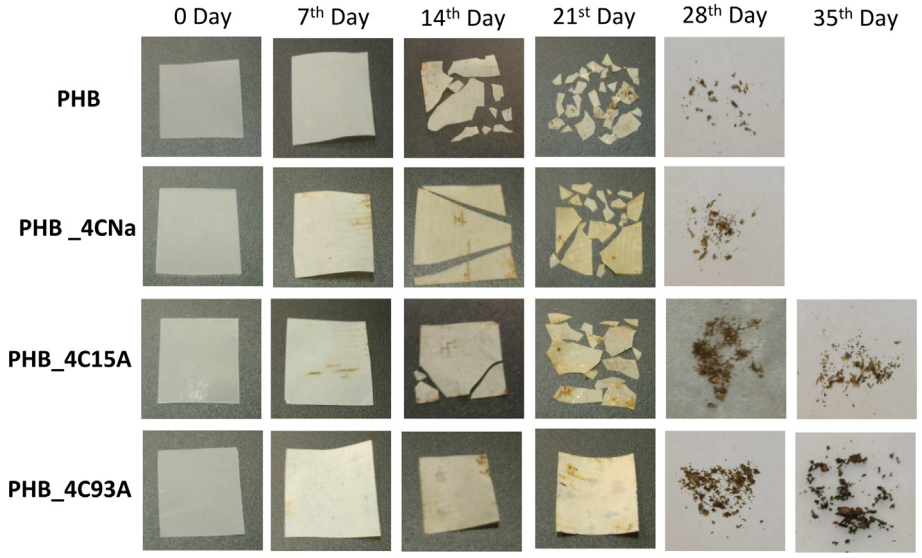

Fig. 5. PHB and PHB nanocomposites before (0 day) and after different stages of disintegration in composting at 58 °C.

the diffusion into the bulk of the film through a more tortuous path [19]. The degraded materials were either digested by the microorganisms or broken into such small fragments that no film residuals could be found in the compost. More material loss and a greater appearance change can be taken to reflect a faster degradation rate. Based on the appearance variations in Fig. 6, the order of disintegration rate can be preliminarily determined as follows: PHB > PHB_4CNa > PHB_4C15A > PHB_4C93A. The enhanced PHB degradation observed with unmodified MMT layered silicates with respect of OMMT modified cloisites had already been reported. It was explained by the presence of Al Lewis acid sites in the inorganic layers [40,41] or by the presence of residual water, due to the hydrophilic nature of the CNa.

The morphology of PHB films containing the different fillers, retrieved regularly from the compost, was characterized by field emission scanning electron microscope. The results are shown in Fig. 7. It can be seen from the FESEM images that the surfaces of PHB films were smooth before degradation while a higher surface roughness characterized the PHB nanocomposite films due to the presence of the fillers. After 7 days of composting, the surfaces of all PHB films were eroded with an evident surface irregularity, and a network of cavities were formed on the surface of PHB_4C93A. FESEM micrographs of specimens exposed for 7 days showed significant number of pits on the surface with the rest of the surface being slightly rougher than the control specimens at start time. However, no cavities appeared on the surfaces of PHB_4C15A and PHB_4CNa. After 28 days of composting, many cavities were formed for all PHB based systems. After 35 days, it was difficult to see the cavities and there are only some PHB fragments [16]. It is very clear from these micrographs that, as a result of bacterial consumption, significant surface erosion takes place in PHB nanocomposites as compared to that in neat PHB. In soil, the surface of the samples became matte initially and then progressively rougher with incubation time, with degradation taking place on all surfaces. When

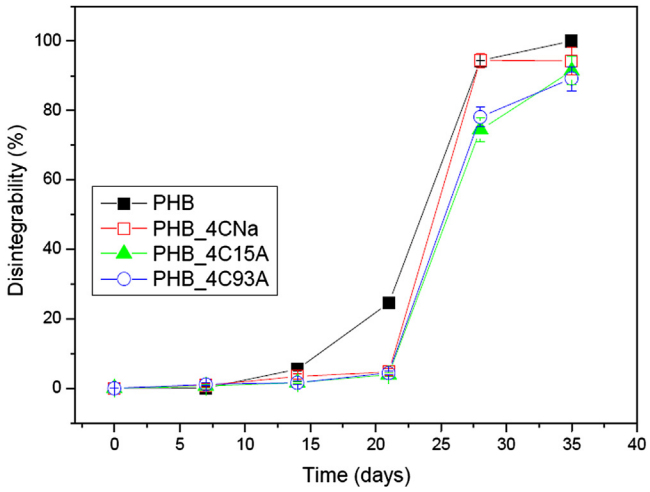

Fig. 6. Disintegrability values of PHB and PHB nanocomposites at different stages of incubation in composting.

the polymer is degraded by extracellular enzymes produced by fungi or other micro-organisms, only the surface is attacked due to the larger size of the enzyme. These differences have also been observed by Doi et al., 1990 [42] where SEM photographs of enzymatically degraded PHB show a very irregular surface although the cross-section of the same sample shows no degradation. Atkinson et al., 1996 [43] observed that the microorganism sub-populations (colonies) grew initially, reached an equilibrium, and decreased eventually in a sawdust compost medium similar to the one used in this study. This could well explain the kinds of topographic patterns of degraded PHB specimens observed in the present study. In the initial composting period, there existed a few microorganism colonies that were spread far apart. As the colonies multiplied, the number of pits increased and spread over other regions of the specimens [44]. The order of disintegration rate determined from the FESEM analysis was in accord with the visual observation (Fig. 5) and disintegrability investigations (Fig. 6).

The FT-IR spectra of PHB and PHB nanocomposites before composting and after 7, 14, 21, 28 and 35 days of degradation were performed. Fig. 8a shows the spectra of PHB where the band at 1724 cm^{-1}, assigned to C═O stretching vibration of carbonyl groups, became wider along the degradation process. The characteristic absorptions of CH_3 out of plane bending, C–O–H in plane bending and C–O stretching vibration were found at 1455, 1377, 1226 and 1183 cm^{-1}. During degradation, the intensity of the above bands became stronger up to 21 days, and at this time the biodegradation rate suddenly change (see Fig. 6) and the peaks almost disappeared, indicating a progressive degradation of the PHB matrix. It can be seen that PHB and PHB composites films had similar absorption peaks in their FT-IR spectra up to 21 days (Fig. 8b shows the spectra of PHB/C15A as an example). The changes in the height of the characteristic peaks were also observed in the case of nanocomposites but some differences arisen. These differences for the OMMT based PHB nanocomposites are visible at 28 and 35 days of composting experiment where the broad peak appeared at 1040 cm^{-1} could show the presence of clay (Si–O stretch). Additionally, the band at 1650 cm^{-1} may be associated to the –C═C– stretching vibration present in the products of degradation formed from the break of the ester link [45–47]. Since the chemical structure of residual PHB was not changed during the degradation process, FT-IR results confirmed that erosion of PHB films, caused by microorganisms action, originated from the surface layer and then spread gradually to the interior of the PHB film [16]. This suggests that no degradation by-products were left on the surface of the specimens after washing with deionized water. The smaller molecules (oligomeric species) formed by chain scission are believed to have leached out into the composting medium or washed.

Fig. 9 shows the DSC thermograms (a,b) of the second heating scan for PHB and PHB nanocomposites, respectively, at 7 and 21

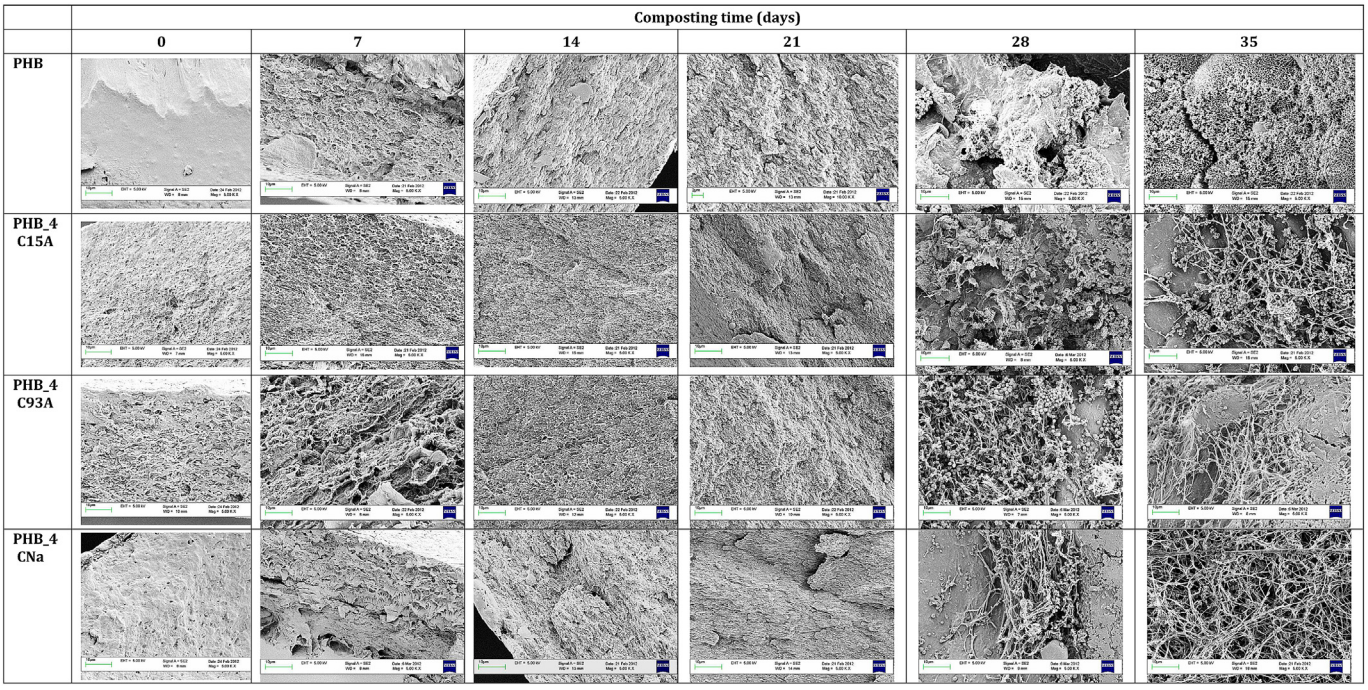

Fig. 7. FESEM images of PHB and PHB nanocomposite surfaces after disintegration in composting at 58 °C.

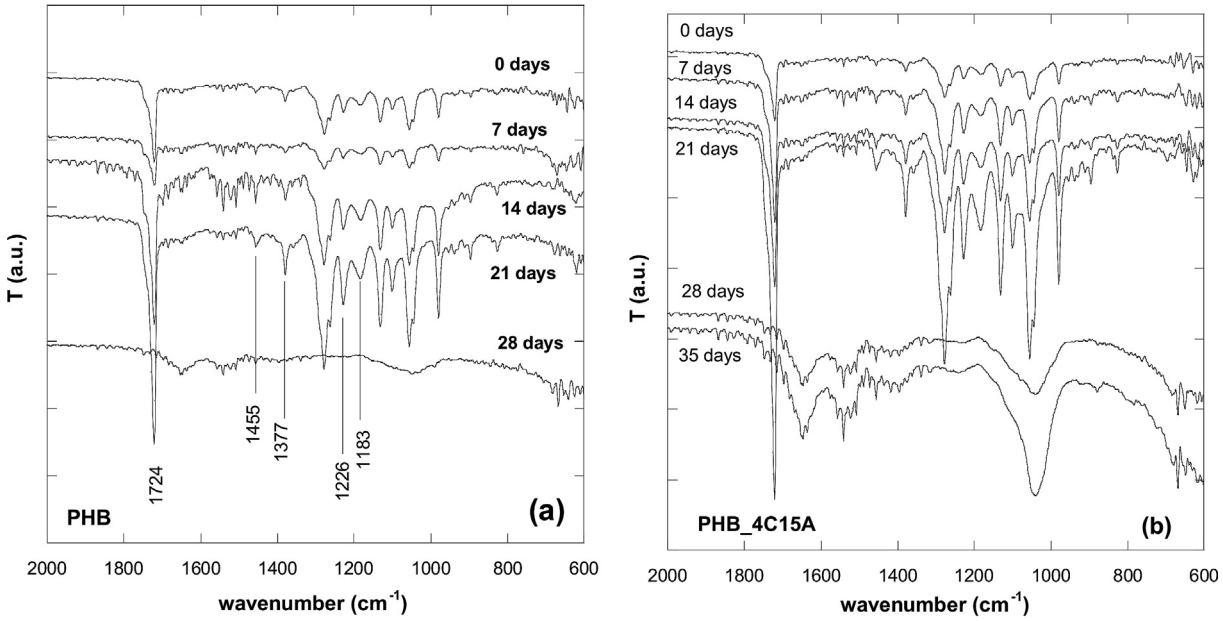

Fig. 8. Infrared spectra of PHB (a) and PHB_4C15A nanocomposite (b) before and after different stages of disintegration in composting.

days of degradation, while in Fig. 9 c and d the DTG curves of the materials at the same conditions, are reported. All the data related to melting and crystallization events measured from DSC tests and the peak temperatures and residual mass obtained from TGA analysis, at 7, 14 and 21 days, are reported in Table 3. It should be pointed out that no data for calorimetric and thermogravimetric tests are reported in Table 3, since no significant thermal events were recorded in the second heating scan due to the degradation of PHB matrix after 28 days of composting test. After 7 days of degradation, melting temperatures decrease with respect to their initial values as a consequence of a molecular chain degradation in composting, according to morphological observations (Table 3). For all samples, the decrease of transition temperatures was evident, however, the great difference in thermal stability of the system was detected for the PHB_4CNa system, for which an evident decrease in crystallization degree was evident. After 21 days in compost, a decrease of the T_{m1} and T_{m2} values was observed for all the samples, due to an increase in the polymer chain mobility for a plasticizing effect of oligomers formed on degradation. In general, the results indicate that crystallinity of the PHB nanocomposites at the different composting times, was not affected by composting conditions. This again suggests that, up to 21 days, degradation during composting occurs at the surface and does not discriminate between crystalline and amorphous states [48,49].

DTG curves of PHB and PHB nanocomposites at different times in composting (7 and 21 days) are shown in Fig. 9 c and d, while the maximum degradation temperatures (T_{peak}) and the residual mass at 600 °C are reported for 7, 14 and 21 days in Table 3. A complete weight loss in a single step was detected for neat PHB and a similar behavior was found after degradation in compost for all the materials. A common shift to higher temperatures was observed at 14 days of incubation, indicating that even after degradation in compost, the introduction of organomodified clays improve the thermal stability of neat PHB, acting as thermal barriers [16]. In the case of CNa, the thermal resistance of PHB slightly decreased, due to the catalytic activity of the Al Lewis acid sites of MMT, as previously reported for the same systems before degradation tests [36]. It can be also observed that the nanocomposites showed, even after degradation tests, higher residual mass than the PHB, due to the presence of inorganic compounds and the PHB_4CNa system showed higher amount of residual mass than the other nanocomposites at the different composting times. The results coming from degradation test in compost confirm that the dispersed silicates in the PHB matrix lower the disintegration rate of the neat polymer, and this effect could be explained by considering the increase in effective path length and time for the microorganism for diffusion into the bulk of the film. Moreover, the presence of dispersed large aspect ratio silicates in the polymer matrix is able to improve the barrier properties and, at the same time, the thermal stability of the different systems up to 21 days of composting test. After three weeks of exposure, the rate of degradation for the PHB_4CNa system is analogous to the neat matrix and much higher if compared to the other nanocomposites and this behavior can be justified with the presence of Al Lewis acid sites in the octahedral layers of montmorillonite and surface hydroxyl groups, which catalyze the hydrolysis of the ester linkages in the polymer.

4. Conclusions

PHB based nanocomposites were successfully produced by solution process adding both unmodified montmorillonite Cloisite Na^+ (CNa) and chemically modified Cloisite 15A and 93A (C15A and C93A) at 4 wt% respect to the polymer matrix. XRD analysis suggests that the PHB crystalline lattice does not change appreciably in the presence of the different montmorillonites while a better dispersion of C15A and C93A in PHB was detected respect to the unmodified clay. Contact angle measurements showed that the composites containing the organically modified OMMT fillers presented a higher hydrophobic nature than the PHB, because of the non-polar modifiers added to C15A and C93A clays. However, thermal investigation revealed no significant changes in the fusion temperature and percentage of crystallinity with the clay addition because the MMT was predominantly in the amorphous phase. The lab-scale composting test showed that all the studied materials were visibly disintegrated after 28 days, while PHB_4C15A and PHB_4C93A formulations were still present at 35 days in composting. The disintegrability values suggest the following order of disintegration: PHB > PHB_4CNa > PHB_4C15A > PHB_4C93A underlining that after

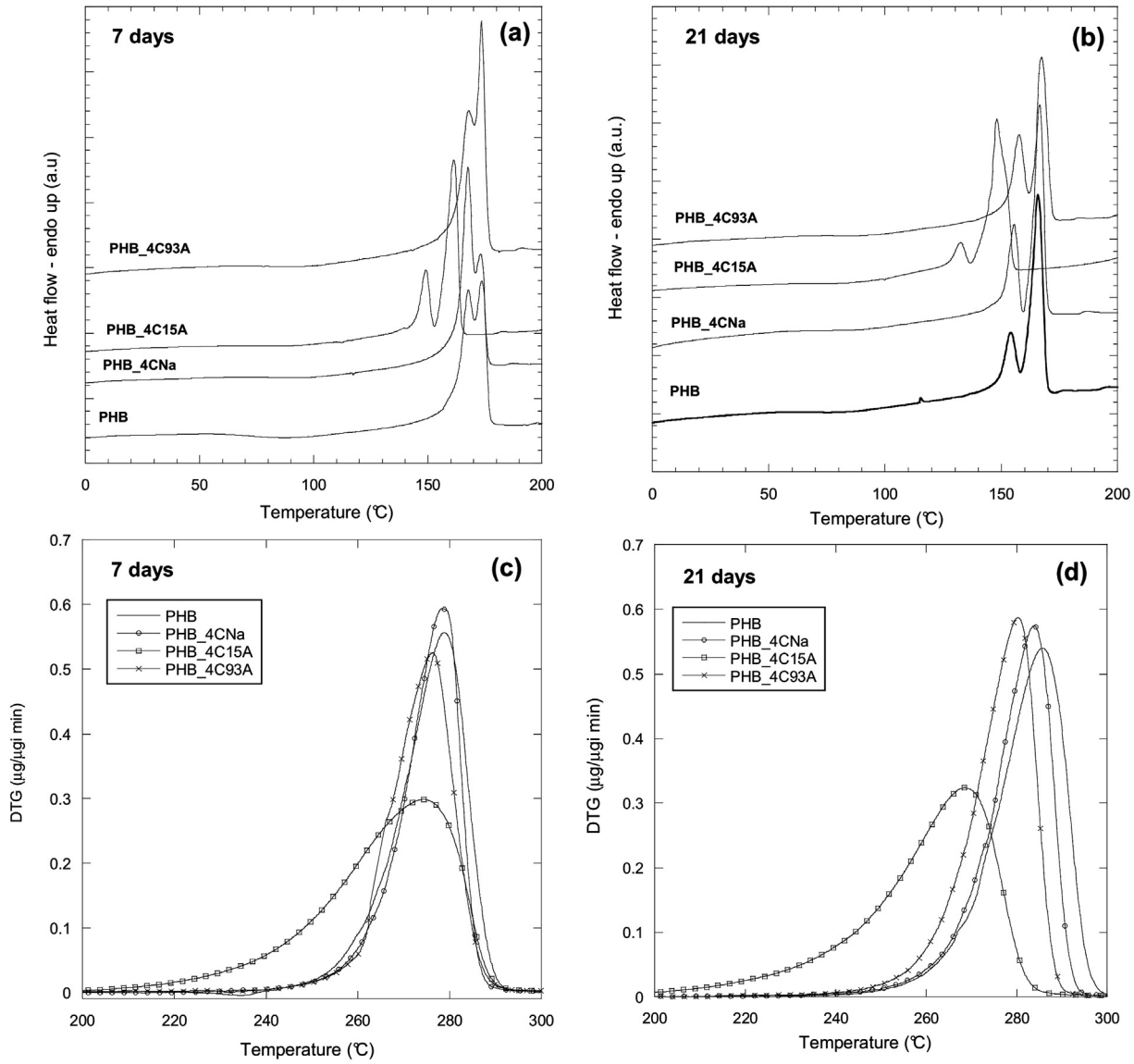

Fig. 9. DSC thermograms at second heating scan (a,b) and derivative curves extracted from TGA analysis (c,d) of PHB and PHB nanocomposites at 7 and 21 days of incubation in composting conditions.

Table 3
Thermal characteristics calculated for the PHB and its nanocomposites from DSC thermograms (cooling and 2nd heating scan) and TGA results at different composting times (7, 14 and 21 days).

	Cooling scan		2nd heating scan						TGA	
	ΔH_c (J/g)	T_c (°C)	T_{cc} (°C)	ΔH_{cc} (J/g)	ΔH_m (J/g)	T_{m1} (°C)	T_{m2} (°C)	X_m (%)	T_{peak} (°C)	Residual mass (%) @ 600 °C
PHB_7d	64.7 ± 2.2	76.3 ± 0.5	91.1 ± 0.1	12.2 ± 3.1	85.8 ± 3.1	167.7 ± 0.3	173.7 ± 0.1	50.4 ± 4.3	278.9 ± 1.5	0.37
PHB_4CNa_7d	69.0 ± 4.2	89.9 ± 2.2	97.2 ± 2.5	10.1 ± 1.5	79.5 ± 7.2	167.8 ± 0.5	175.3 ± 1.6	45.7 ± 5.7	278.5 ± 2.1	6.44
PHB_4C15A_7d	74.7 ± 9.2	86.1 ± 1.2	92.6 ± 2.6	4.4 ± 2.2	87.4 ± 2.4	149.3 ± 1.1	163.1 ± 2.6	54.6 ± 2.6	274.6 ± 1.7	2.94
PHB_4C93A_7d	78.2 ± 8.9	89.3 ± 0.2	98.6 ± 1.2	7.3 ± 1.8	91.3 ± 8.0	167.6 ± 0.2	173.6 ± 0.1	55.3 ± 4.1	276.3 ± 1.8	2.08
PHB_14d	61.4 ± 0.5	70.3 ± 0.1	91.2 ± 1.2	7.2 ± 2.6	85.4 ± 2.1	171.7 ± 1.4	160.0 ± 1.5	53.6 ± 0.4	277.2 ± 0.4	0.41
PHB_4CNa_14d	61.6 ± 4.7	89.4 ± 6.3	95.2 ± 0.3	5.0 ± 1.5	74.6 ± 7.4	161.6 ± 0.3	172.4 ± 1.5	45.8 ± 4.0	286.5 ± 1.3	3.60
PHB_4C15A_14d	72.4 ± 2.0	79.3 ± 2.4	92.3 ± 4.4	6.1 ± 1.2	80.8 ± 1.5	142.2 ± 3.2	160.7 ± 1.5	49.2 ± 2.6	279.3 ± 2.3	1.53
PHB_4C93A_14d	74.28 ± 4.0	89.2 ± 0.5	96.2 ± 2.0	6.6 ± 1.0	86.0 ± 3 0	168.1 ± 4.9	175.4 ± 0.1	52.2 ± 1.3	275.8 ± 2.6	2.20
PHB_21d	66.1 ± 0.3	69.7 ± 1.5	91.5 ± 3.1	4.5 ± 0.5	77.7 ± 5.0	152.0 ± 3.0	167.5 ± 2.6	50.1 ± 0.3	285.8 ± 3.0	0.53
PHB_4CNa_21d	71.4 ± 0.4	76.6 ± 7.6	87.5 ± 2.9	5.1 ± 0.6	86.8 ± 4.3	152.1 ± 3.0	167.2 ± 3.5	53.7 ± 3.3	283.9 ± 2.5	4.13
PHB_4C15A_21d	67.1 ± 3.4	70.2 ± 6.1	80.4 ± 3.0	5.0 ± 1.1	76.7 ± 2.0	127.3 ± 1.6	152.8 ± 3.1	47.2 ± 1.9	268.3 ± 2.0	2.93
PHB_4C93A_21d	70.0 ± 2.0	81.8 ± 6.0	88.6 ± 3.6	6.2±1.0	87.4 ± 3.6	155.4 ± 2.9	170.2 ± 2.3	53.4 ± 3.0	280.3 ± 2.5	1.83

three weeks of exposure, the rate of biodegradation for the PHB_4CNa system is analogous to the neat matrix and much higher if compared to the other nanocomposites. The results revealed that the biodegradation is influenced by several factors including the crystallinity and hydrophobicity of the material, dispersion, antimicrobial and acid properties of the fillers. Then, the study underlined the effect of clay organic modification on the structural properties and disintegrability rate of PHB nanocomposites opening perspective to modulate the disintegration pattern selecting a filler with specific characteristics.

Acknowledgments

The authors gratefully acknowledge the support from the National Research Council of Argentina (CONICET) – PIP 014 and the National University of Mar del Plata. The Author Elena Fortunati is the recipient of the fellowship "L'Oreal Italia per le Donne e la Scienza 2012" for the project "Progettazione, sviluppo e caratterizzazione di biomateriali nanostrutturati capaci di modulare la risposta e il differenziamento delle cellule staminali". The Authors acknowledge Gesenu S.p.a. for compost supply.

References

[1] Bordes P, Polelt E, Bourbigot S, Avérous L. Structure and properties of PHA/clay nano-biocomposites prepared by melt intercalation. Macromol Chem Phys 2008;209:1473–84.
[2] Grassie N, Murray EJ, Holmes PA. Thermal degradation of poly(-(D)-beta-hydroxybutyric acid): part 1-identification and quantitative analysis of products. Polym Degrad Stab 1984;6(1):47–61.
[3] Lim YT, Park OO. Phase morphology and rheological behavior of polymer/layered silicate nanocomposites. Rheologica Acta 2001;40:220–9.
[4] Cyras VP, Manfredi LB, Ton-That MT, Vazquez A. Physical and mechanical properties of thermoplastic starch/montmorillonite nanocomposite films. Carbohydr Polym 2008;73:55–6.
[5] Choi WM, Kim TW, Park OO, Chang YK, Lee JW. Preparation and characterization of poly (hydroxy-butyrate-co-hydroxyvalerate)-clay nanocomposite. J Appl Polym Sci 2008;90:525–9.
[6] Lim ST, Hyun YH, Lee CH, Choi HJ. Preparation and characterization of microbial biodegradable poly(3-hydroxybutyrate)/organoclay nanocomposite. J Mater Sci Lett 2003;22:299–302.
[7] Yano K, Usuki A, Okada A. Synthesis and properties of polyimide-clay hybrid films. J Polym Sci Part A Polym Chem 1997;35:2289–94.
[8] Xu RJ, Manias E, Snyder AJ, Runt J. New biomedical poly(urethane urea)–layered silicate nanocomposites. Macromolecules 2001;34:337–9.
[9] Okada A, Usuki A. The chemistry of polymer-clay hybrids. Mater Sci Eng C 1995;3:109–15.
[10] Pantani R, Sorrentino A. Influence of crystallinity on the biodegradation rate of injection-moulded poly(lactic acid) samples in controlled composting conditions. Polym Degrad Stab 2013;98(5):1089–96.
[11] Bikiaris DN. Polym Degrad Stab 2013. http://dx.doi.org/10.1016/j.polymdegradstab.2013.05.016.
[12] Bordes P, Hablot E, Pollet E, Averous L. Effect of clay organomodifiers on degradation of polyhydroxyalkanoates. Polym Degrad Stab 2009;94:789–96.
[13] Botana A, Mollo M, Eisenberg P, Torres Sanchez RM. Effect of modified montmorillonite on biodegradable PHB nanocomposites. Appl Clay Sci 01/2010;27:263.
[14] Gutierrez-Wing MT, Stevens BE, Theegala CS, Negulescu II, Rusch KA. Aerobic biodegradation of polyhydroxybutyrate in compost. Environ Eng Sci 2011;28(7):477–88.
[15] Weng YX, Wang XL, Wang YZ. Biodegradation behavior of PHAs with different chemical structures under controlled composting conditions. Polym Test 2011;30(4):372–80.
[16] Weng YX, Wang Y, Wang XL, Wang YZ. Biodegradation behavior of PHBV films in a pilot-scale composting conditions. Polym Test 2010;29(5):579–87.
[17] Maiti P, Batt CA, Giannelis EP. Renewable plastics: synthesis and properties of PHB nanocomposites. Polym Mater Sci Eng 2003;88:58–9.
[18] Maiti P, Batt CA, Giannelis EP. New biodegradable polyhydroxybutyrate/layered silicate nanocomposites. Biomacromolecules 2007;8(11):3393–400.
[19] Wang S, Song C, Chen GT, Guo T, Liu J, Zhang B, et al. Characteristics and biodegradation properties of poly(3-hydroxybutyrate-co-3-hydroxyvalerate)/organophilic montmorillonite (PHBV/OMMT) nanocomposite. Polym Degrad Stab 2005;87:69–76.
[20] Lai M, Li J, Yang J, Liu J, Tong X, Cheng H. The morphology and thermal properties of multi-walled carbon nanotube and poly(hydroxybutyrate-co-hydroxyvalerate)composite. Polym Int 2004;53:1479–84.
[21] Sanchez-Garcia MD, Lagaron JM, Hoa SV. Effect of addition of carbon nanofibers and carbon nanotubes on properties of thermoplastic biopolymers. Compos Sci Technol 2010;70:1095–105.
[22] Jing X, Qui Z. Crystallization kinetics and thermal property of biodegradable poly(3-hydroxybutyrate)/graphene oxide nanocomposites. J Nanosci Nanotechnol 2012;12:7314–21.
[23] Jing X, Qiu Z. Effect of low thermally reduced graphene loadings on the crystallization kinetics and morphology of biodegradable poly(3-hydroxybutyrate). Ind Eng Chem Res 2012;51:13686–91.
[24] Luo S, Netravali AN. A study of physical and mechanical properties of poly(hydroxybutyrate-co-hydroxyvalerate) during composting. Polym Degrad Stab 2003;80(1):59–66.
[25] Lotto NT, Calil MR, Guedes CGF, Rosa DS. The effect of temperature on the biodegradation test. Mater Sci Eng C 2004;24:659–62.
[26] Narendra KS, Das Purkayastha BP, Roy JK, Banik RM, Gonugunta P, Misrad M, et al. Tuned biodegradation using poly(hydroxybutyrate-co-valerate) nanobiohybrids: emerging biomaterials for tissue engineering and drug delivery. J Mater Chem 2011;21:15919–27.
[27] Cyras VP, Rozsa C, Galego N, Vázquez A. Kinetic expression for the isothermal crystallization of P(HB-HV). J Appl Polym Sci 2004;94:1657–61.
[28] Chiu HJ. Segregation morphology of poly(3-hydroxybutyrate)/poly(vinyl acetate) and poly(3-hydroxybutyrate-co-10% 3-hydroxyvalerate)/poly(vinyl acetate) blends as studied via small angle X-ray scattering. Polymer 2005;46:3906–13.
[29] Hurrell BL, Cameron RE. A wide-angle X-ray scattering study of the ageing of poly(hydroxybutyrate). J Mater Sci 1998;33(7):1709–13.
[30] Salehabadi A, Bakar MA. Poly(3-hydroxybutyrate)–organo modified montmorillonite nanohybrid; preparation and characterization. Adv Mat Res 2012;622–623:263–70.
[31] Da Silva Moreira Thiré RM, Cardoso Arruda L, Silva Barreto L. Morphology and thermal properties of poly(3-hydroxybutyrate-co-3-hydroxyvalerate)/attapulgite nanocomposites. Mater Res 2011;14(3):340–4.
[32] Pluta M, Galeski A, Alexandre M, Paul MA, Dubois P. Polylactide/montmorillonite nanocomposites and microcomposites prepared by melt blending: structure and some physical properties. J Appl Polym Sci 2002;86:1497–506.
[33] Wang YW, Zhang R, Li Q, Shen C. Preparation and characterization of microbial biodegradable poly(3-hydroxybutyrate-co-4-hydroxybutyrate)/organoclay nanocomposites. Polym Compos 2012;33:838–42.
[34] Pearce R, Marchessault RH. Multiple melting in blends of isotactic and atactic poly(β-hydroxybutyrate. Polymer 1994;35:3990.
[35] D'Amico DA, Manfredi LB, Cyras VP. Crystallization behavior of poly(3-hydroxybutyrate) nanocomposites based on modified clays: effect of organic modifiers. Thermochim Acta 2012;544(20):47–53.
[36] D'Amico DA, Manfredi LB, Cyras VP. Relationship between thermal properties, morphology, and crystallinity of nanocomposites based on polyhydroxybutyrate. J Appl Polym Sci 2012;123:200–8.
[37] Di Maio E, Iannace S, Sorrentino L, Nicolais L. Isothermal crystallization in PCL/clay nanocomposites investigated with thermal and rheometric methods. Polymer 2004;45(26):8893–900.
[38] Chivrac F, Pollet E, Averous L. Nonisothermal crystallization behavior of poly(butylene adipate-co-terephthalate)/clay nano-biocomposites. J Polym Sci Polym Phys 2007;45(13):1503–10.
[39] Li S, Girard A, Garreau H, Vert M. Enzymatic degradation of polylactide stereocopolymers with predominant d-lactyl contents. Polym Degrad Stab 2001;71:61–7.
[40] Xie W, Gao Z, Pan WP, Hunter D, Singh A, Vaia R. Thermal degradation chemistry of alkyl quaternary ammonium montmorillonite. Chem Mater 2001;13(9):2979–90.
[41] Pandey JK, Kumar AP, Misra M, Mohanty AK, Drzal LT, Singh RP. Recent advances in biodegradable nanocomposites. J Nanosci Nanotechnol 2005;5(4):497–526.
[42] Doi Y, Kanesawa Y, Kunioka M, Saito T. Biodegradation of microbial copolyesters: poly(3-hydroxybutyrate-co-3-hydroxyvalerate) and poly(3-hydroxybutyrate-co-4-hydroxybutyrate). Macromolecules 1990;23:26–31.
[43] Atkinson CF, Jones DD, Gauthier JJ. Biodegradability and microbial activities during composting of poultry litter. Poultry Sci 1996;75:608–17.
[44] Nobes GAR, Marchessault RH, Chanzy H, Briese BH, Jendrossek D. Splintering of poly(3-hydroxybutyrate) single crystals by PHB-depolymerase a from *Pseudomonas lemoignei*. Macromolecules 1996;29:8330–3.
[45] Mousavioun P, George GA, Doherty WOS. Environmental degradation of lignin/poly(hydroxybutyrate) blends. Polym Degrad Stab 2012;97(7):1114–22.
[46] Rodríguez-Contreras A, Calafell-Monfort M, Marqués-Calvo MS. Enzymatic degradation of poly(3-hydroxybutyrate-co-4-hydroxybutyrate) by commercial lipases. Polym Degrad Stab 2012;97:597–604.
[47] Cyras VP, Vazquez A, Rozsa C, Fernandez NG, Torre L, Kenny JM. Thermal stability of P(HB-co-HV) and its blends with polyalcohols: crystallinity, mechanical properties and kinetic of degradation. J Appl Polym Sci 2000:2889–900.
[48] Calil MR, Guedes CGF, Rosa DS. Biodegradation behavior of PHBV films in a pilot-scale composting condition. Mater Sci Eng 2004;24:659–62.
[49] Achilias DS, Panayotidou E, Zuburtikudis I. Thermal degradation kinetics and isoconversional analysis of biodegradable poly(3-hydroxybutyrate)/organomodified montmorillonite nanocomposites. Thermochim Acta 2011;514:58–66.